ARMY RESEARCH LABORATORY

Rare-earth Doped GaN – An Innovative Path Toward Area-scalable Solid-state High Energy Lasers Without Thermal Distortion (2nd year)

by Michael Wraback and Mark Dubinskiy

ARL-TR-5213 **June 2010**

NOTICES

Disclaimers

The findings in this report are not to be construed as an official Department of the Army position unless so designated by other authorized documents.

Citation of manufacturer's or trade names does not constitute an official endorsement or approval of the use thereof.

Destroy this report when it is no longer needed. Do not return it to the originator.

Army Research Laboratory
Adelphi, MD 20783-1197

ARL-TR-5213 **June 2010**

Rare-earth Doped GaN – An Innovative Path Toward Area-scalable Solid-state High Energy Lasers Without Thermal Distortion (2nd year)

Michael Wraback and Mark Dubinskiy
Sensors and Electron Devices Directorate, ARL

REPORT DOCUMENTATION PAGE

Form Approved
OMB No. 0704-0188

1. REPORT DATE *(DD-MM-YYYY)*	2. REPORT TYPE	3. DATES COVERED (From - To)
June 2010	DRI	

4. TITLE AND SUBTITLE
Rare-earth Doped GaN – An Innovative Path Toward Area-scalable Solid-state High Energy Lasers Without Thermal Distortion (2nd year)

5a. CONTRACT NUMBER

5b. GRANT NUMBER

5c. PROGRAM ELEMENT NUMBER

6. AUTHOR(S)
Michael Wraback and Mark Dubinskiy

5d. PROJECT NUMBER

5e. TASK NUMBER

5f. WORK UNIT NUMBER

7. PERFORMING ORGANIZATION NAME(S) AND ADDRESS(ES)
U.S. Army Research Laboratory
ATTN: RDRL-SEE-M
2800 Powder Mill Road
Adelphi, MD 20783-1197

8. PERFORMING ORGANIZATION REPORT NUMBER
ARL-TR-5213

9. SPONSORING/MONITORING AGENCY NAME(S) AND ADDRESS(ES)

10. SPONSOR/MONITOR'S ACRONYM(S)

11. SPONSOR/MONITOR'S REPORT NUMBER(S)

12. DISTRIBUTION/AVAILABILITY STATEMENT
Approved for public release; distribution unlimited.

13. SUPPLEMENTARY NOTES

14. ABSTRACT
In situ neodymium (Nd) doping of gallium nitride (GaN) and aluminum nitride (AlN) by plasma-assisted molecular beam epitaxy (PA-MBE) has been demonstrated for the first time. For GaN, Nd doping as high as ~8 at.% has been demonstrated, with no evidence of phase segregation identified by x-ray diffraction (XRD) for Nd up to ~1 at.%. The strongest room-temperature luminescence was observed for a doping level between 0.1–1 at.%. The Stark energy levels of the three characteristic Nd emission multiplets were resolved by photoluminescence (PL) and photoluminescence excitation (PLE) spectroscopy. The enhanced substitutional doping at the gallium (Ga) site and low optical loss in waveguide structures suggests that GaN:Nd may have significant potential for use in simple, area-scalable, room-temperature, diode-pumped solid-state high energy lasers (HELs). Next-generation devices may be able to take advantage of the improved thermal conductivity of an AlN host.

15. SUBJECT TERMS
GaN, AlN, Nd, high energy laser, thermal conductivity

16. SECURITY CLASSIFICATION OF:			17. LIMITATION OF ABSTRACT	18. NUMBER OF PAGES	19a. NAME OF RESPONSIBLE PERSON
a. REPORT	b. ABSTRACT	c. THIS PAGE			Michael Wraback
Unclassified	Unclassified	Unclassified	UU	28	19b. TELEPHONE NUMBER (*Include area code*) (301) 394-1459

Standard Form 298 (Rev. 8/98)
Prescribed by ANSI Std. Z39.18

Contents

List of Figures iv

List of Tables iv

Acknowledgments v

1. Objective 1

2. Approach 1

3. Results 2

3.1 Growth of Nd Doped GaN by MBE....2

3.2 Optical Studies of Nd Doped GaN....4

3.3 Optical Studies of Nd Doped AlN....12

4. Conclusions 13

5. References 14

6. Transitions 16

6.1 Publications....16

6.2 Presentations....16

List of Symbols, Abbrviations, and Acronyms 18

Distribution List 19

List of Figures

Figure 1. (a) Nd atomic percent and PL intensity versus Nd cell temperature and (b) GaN transmission at 600 nm as a function of Nd concentration. The reduced sample transmission is due to the rough back side.....3

Figure 2. X-ray data for GaN:Nd at 1 at% and 8 at% Nd in the GaN film.....4

Figure 3. Nd at% obtained by SIMS as a function of Nd cell temperature for two Ga fluxes: Ga = 1.5×10^{-7} torr BEP (blue) and Ga= 3.5×10^{-7} torr BEP (red). 4

Figure 4. Room-temperature (300 K) and low-temperature (~30 K) PL spectra in logarithmic scale from GaN:Nd optically excited at 836 nm. Transitions from the lower and upper levels of the $^4F_{3/2}$ excited state to the *m*th Stark level of the $^4I_{9/2}$, $^4I_{11/2}$, and $^4I_{13/2}$ levels and RE-related (marked with an arrow) phonon sidebands are labeled. 6

Figure 5. Low-temperature (~30 K) PL spectra in logarithmic scale from GaN:Nd optically excited below and above the bandgap at 836 nm and 325 nm, respectively. Longitudinal optical (LO) and transverse optical (TO) phonon sidebands are labeled. Peaks marked with a downward arrow indicate plasma lines from the 325-nm laser. 7

Figure 6. PL excitation spectra in logarithmic scale from GaN:Nd measured at the 1106 nm emission line at ~13 and ~150 K. Transitions from the lowest two levels of the $^4I_{9/2}$ ground state to the *m*th Stark level of the $^4F_{5/2}$, $^2H_{9/2}$, $^4F_{7/2}$, and $^4S_{3/2}$ levels, as well as LO and TO phonon replicas are labeled.....9

Figure 7. Optical loss at emission energy 1.12 eV (1106 nm) measured using the SES technique. The solid line is a fit of the experimental data (open circles) according to equation 1.....11

Figure 8. Output intensity versus excitation length measured at emission energy 1.12 eV (1106 nm). The solid line is a fit of the experimental data (open circles) according to equation 2.....12

Figure 9. PL from Nd doped AlN as a function of growth temperature and Al flux for $^4F_{3/2}$ to $^4I_{11/2}$ transitions.....13

List of Tables

Table 1. Energy of the crystal field-split levels of Nd^{3+} ions in GaN for the main incorporation site as determined by PL, PLE, and CEES (in parenthesis) measurements. 10

Acknowledgments

We would like to thank Eric Readinger for growth and physical characterization of the neodymium (Nd) doped gallium nitride (GaN) and helpful discussions; Grace Metcalfe, Keith Graham, and Larry Merkle for optical characterization and helpful discussions; and John Gruber for theoretical modeling and helpful discussions.

INTENTIONALLY LEFT BLANK.

1. Objective

The objective of this effort was to develop a qualitatively new approach to highly scalable diode-pumped solid-state lasers based on rare-earth (RE) neodymium (Nd^{3+}) doping of gallium nitride (GaN), a high thermal conductivity material, with the goal of fully eliminating the bottleneck in the heat removal process associated with the low thermal conductivity of the gain medium compared to that of heat-sinking materials.

2. Approach

Laser-based directed energy weapons (DEWs) are important components for future Army missile defense systems. The diode-pumped, RE-doped, solid-state laser is a very promising path towards achieving a DEW-sufficient level of average power from a reasonably compact device, but the extreme pump power densities, combined with the inevitable non-radiative losses in the pump-lase process, introduce severe thermal loading in the gain medium. Regardless of the sophistication of heat removal technique and its efficiency, the gain medium itself is the bottleneck for non-distortive heat removal—simply due to low thermal conductivity of known gain media compared to that of heat-sinking material. The best known laser hosts, e.g., yttrium aluminum garnet (YAG), possess thermal conductivities (10–11 W/(m-K)) that are ~1.5 orders of magnitude lower than those of known heat-sinking materials. In order to eliminate this technical hurdle, an innovative gain medium—with thermal conductivity on the same order as copper (~390 W/(m-K))—has to be engineered.

The approach pursued in this work is based on RE doping of GaN, in particular, Nd^{3+}-doped GaN, with a room temperature (RT) thermal conductivity (131 to 200 W/(m-K)), which is 10 to 15 times higher than that of Nd:YAG and 20 to 30 times higher than that of Nd: yttrium lithium fluoride (YLF). RE-doped GaN laser development, if successful, would be a breakthrough toward simple, area-scalable, room-temperature (as opposed to cryogenically cooled) solid-state high-energy lasers (HELs) with nearly zero thermal distortions, eliminating the need for sophisticated heat management. After Favennec et al. (*1*) demonstrated a reduction in thermal quenching in erbium (Er)-doped materials with increasing bandgap, interest in wide bandgap semiconductors as host materials expanded. In particular, wurtzite GaN has strong ionic bonds that can enhance the intra-$4f^n$ transition probability in the RE^{3+} ion with substitutional occupation of the Ga site. Light emission from GaN doped with europium (Eu), Er, praseodymium (Pr), thulium (Tm), ytterbium (Yb), Nd, and dysprosium (Dy) has been demonstrated by photoluminescence (PL), electroluminescence (EL), and/or cathodoluminescence (CL) (*2*, *3*). As the RE dopant, Nd is an excellent candidate due to its

success in Nd-doped solid-state lasers, which have attained power levels higher than that from any other four-level material (*4*). Nd has been incorporated into GaN through ion-implantation (*5*) and reactive co-sputtering (*6*). Ion-implantation creates doping profiles and damage effects that often require a post implantation anneal due to the amorphization of the GaN lattice; however, annealing does not completely recover the damage. GaN ion implanted with Nd finds the majority of Nd^{3+} ions sitting on the Ga substitutional "site"; however, four other "sites" associated with defects are also identified (*5*). For reactive co-sputtering of GaN with RE atoms, a post-growth anneal (≥700 °C) in nitrogen is often necessary for PL emission (*7–9*).

Although PL (*5*) and EL (*7*) from Nd-doped GaN have been observed, the Stark levels of the 4*f* states have never been resolved, partially due to implantation-related damage of the host material and Nd^{3+} ions occupying multiple sites. In this work, in situ doping of GaN with Nd by plasma-assisted molecular beam epitaxy (PA-MBE) is demonstrated for the first time, with enhanced substantial doping at the Ga site (*10*). This growth technique enables the resolution of the Stark energy levels of the Nd^{3+} ion in GaN by PL and photoluminescence excitation (PLE) spectroscopy. The PLE spectroscopy also enables one to define an optimal pumping wavelength amenable to near-IR diode laser pumping that limits thermal losses. Since the GaN:Nd layers grown by MBE are thin (2–5 μm), a guided-wave architecture for edge-pumping the device (which provides the highest level of laser efficiency due to the pump and signal mode confinement within a crystalline-guided structure) has been designed. The successful implementation of this approach could lead to the development of the first diode pumped Nd^{3+}:GaN laser.

3. Results

3.1 Growth of Nd Doped GaN by MBE

GaN samples were grown on sapphire substrates with a fixed growth rate at two temperatures. The Nd cell temperature was varied from 850–1025 °C, and the Ga flux, measured as beam equivalent pressure (BEP), was varied from 9.8×10^{-6} to 5.6×10^{-7} torr. The secondary ion mass spectrometry (SIMS) profiling tracked the Ga and Nd signals and assumed the Ga signal was associated with a fully dense stoichiometric GaN film. The average Nd doping concentration, over the bulk of the film thickness, was converted to Nd atomic percent within the GaN matrix. A maximum Nd concentration of ~8 at.% was demonstrated (figure 1a). Initial work for the incorporation of Nd used nitrogen rich growth, for which the Nd and Ga had little competition for the same lattice site, as excess nitrogen was always present (*10*). These samples produced significant PL intensities of the Nd 4*f* transitions, but only showed limited PL output with low Nd atomic percentages and when Nd atomic percentages were greater than 1. The epilayers with high atomic percent Nd (>1) had extra peaks in the x-ray diffraction (XRD) data, and the transmission and reflectance (not shown) data showed a diminished intensity (figure 1b),

possibly due to Nd clustering or the formation of a second phase. Figure 2 shows typical ω-2θ x-ray scans about the (0002) GaN peak that include the (0006) sapphire peak. The high angle shoulder on the GaN peak (17.27°) is the aluminum nitride (AlN) buffer layer. The typical x-ray rocking curve (XRC) about the GaN (0002) reflection yields a full width at half maximum (FWHM) of ~1400 arcsec, which is consistent with the use of nitrogen rich growth conditions shown to be favorable for RE optical emission from the GaN matrix (*11*). The FWHM of the XRC data for these nitrogen rich films implies a high defect density not ideal for thermal properties (*12*). Subsequent growths were carried out under varying Ga flux conditions, with significant improvement in crystal quality observed under Ga rich conditions (x-ray data not shown). Figure 3 shows Nd concentration obtained from SIMS measurements as a function of Nd cell temperature for two different Ga fluxes during growth. At higher Ga flux, one needs to increase the Nd cell temperature, and therefore the Nd flux, to attain the same amount of Nd in the film. This result suggests that Ga rich growth potentially leads to less Nd incorporation within the matrix, possibly due to the increased competition for that lattice position. Since the maximum Nd flux is limited by the cell design, one possible solution may involve growing in a more nitrogen rich regime using low dislocation GaN substrates to maintain the crystal quality of the GaN:Nd epilayers.

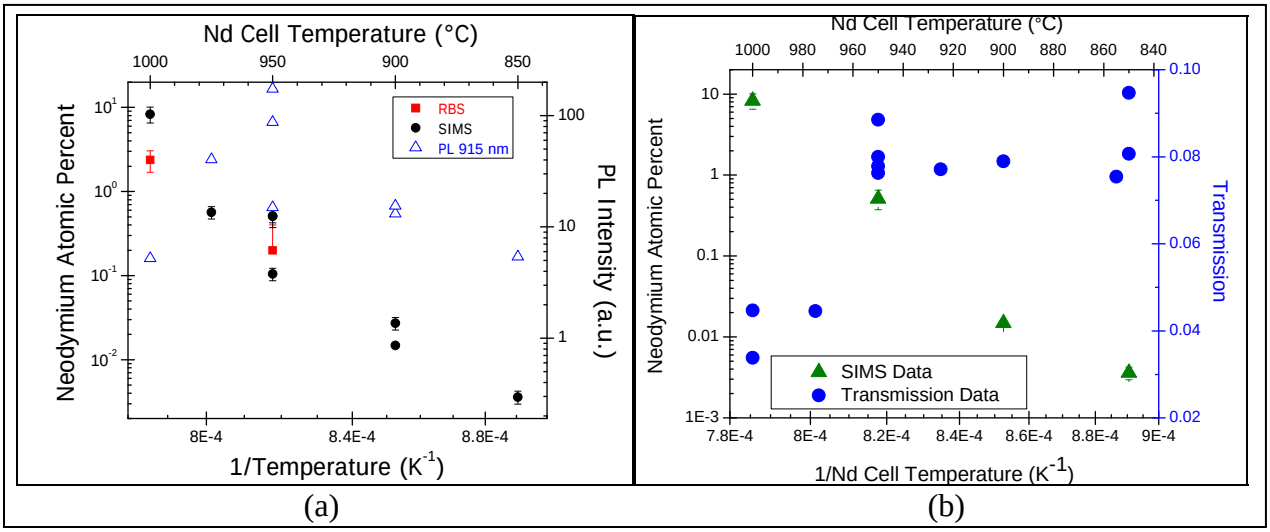

Figure 1. (a) Nd atomic percent and PL intensity vs. Nd cell temperature and (b) GaN transmission at 600 nm as a function of Nd concentration. The reduced sample transmission is due to the rough back side.

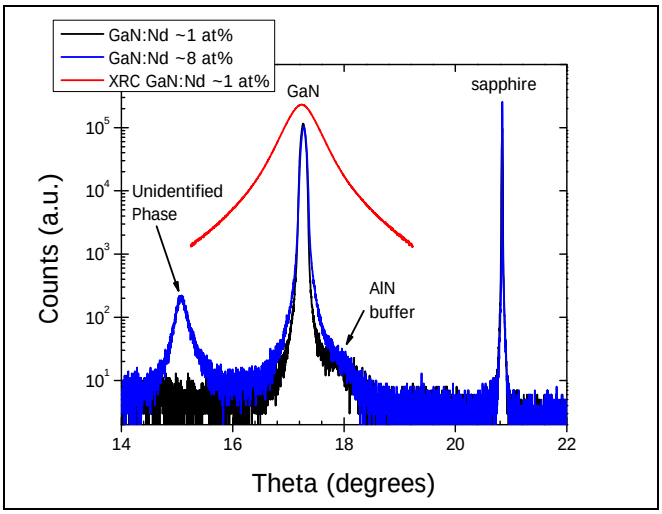

Figure 2. X-ray data for GaN:Nd at 1 and 8 at.% Nd in the GaN film.

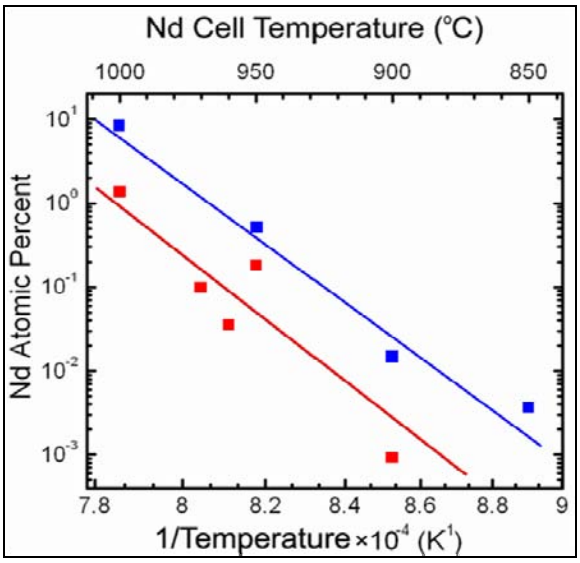

Figure 3. Nd at% obtained by SIMS as a function of Nd cell temperature for two Ga fluxes: Ga = 1.5×10^{-7} torr beam equivalent pressure (blue) and Ga= 3.5×10^{-7} torr BEP (red).

3.2 Optical Studies of Nd Doped GaN

The GaN:Nd samples were mounted in a closed-loop helium cryostat system for temperature dependent PL and PLE measurements. A Nd: yttrium orthovanadate (YVO_4)-pumped continuous wave (CW) Ti:Sapphire laser tunable between 750 to 950 nm and with an excitation density of ~20kW/cm^2 and a CW helium-cadmium (HeCd) laser at 325 nm and with an excitation density of ~0.1kW/cm^2 were used for below and above bandgap excitation, respectively. The resulting luminescence was collected into a 1-m focal length spectrometer and focused onto a liquid nitrogen cooled germanium (Ge) detector.

PL spectra from GaN samples doped with various Nd concentrations show similar spectral features. Figure 4 shows a typical PL spectrum at low temperature (~30 K) from Nd-doped GaN. Strong emission due to transitions from the $^4F_{3/2}$ excited state to the $^4I_{9/2}$, $^4I_{11/2}$, and $^4I_{13/2}$ manifolds in the energy (wavelength) range 1.30–1.36 eV (910–950 nm), 1.08–1.13 eV (1100–1150 nm), 0.84–0.89 eV (1400–1480 nm), respectively, are observed. These Nd transitions are red shifted with respect to the same transitions in a Nd:YAG matrix due to the difference in the GaN crystal field. Also, because of the crystal field experienced by substitutional Nd-ions at Ga sites, there are a total of $J+1/2$ Stark sublevels in each manifold, where J is the total angular momentum. The PL peaks appear in pairs, which are labeled in figure 4 by the integer m that corresponds to the transition from the $^4F_{3/2}$ doublet to the mth Stark component of the $^4I_{9/2}$, $^4I_{11/2}$, and $^4I_{13/2}$ manifolds of the Nd^{3+} ion. The lower (higher) energy PL peak of each pair corresponds to transitions from the ground state (first excited state) Stark level of the $^4F_{3/2}$ excited state. The peaks in each pair are separated by 4.1 meV, indicating the splitting energy of the $^4F_{3/2}$ doublet. The small size of this splitting allows thermal activation of the upper sublevel making the corresponding emission transitions observable even at the lowest temperatures used in our studies. The most intense emission peaks are observed from transitions to the $^4I_{11/2}$ manifold, with the strongest emission line at 1.12 eV (1106 nm) attributed to the transition from the $m = 0$ Stark level of the $^4F_{3/2}$ state to the $m = 0$ Stark level of the $^4I_{11/2}$ manifold. Compared to room-temperature PL spectra, the low-temperature spectra show relatively small (<1 meV) or no shifts in peak energy position, consistent with the 4*f* shell being well shielded from the host material (*13*). The PL intensity of the 1106 nm peak for direct pumping of the $^4F_{3/2} \rightarrow {}^4I_{9/2}$ transition (915 nm) at room temperature increases when increasing Nd up to ~0.5 at.% (figure 1). At higher Nd concentrations, the decrease in PL intensity may be linked to the diminished transmittance and possibly to quenching associated with the closer proximity of Nd atoms (*14*), as suggested by the additional XRD peak in figure 2. This possibility of quenching is also consistent with the observation of non-exponential fluorescence decay following pulsed excitation.

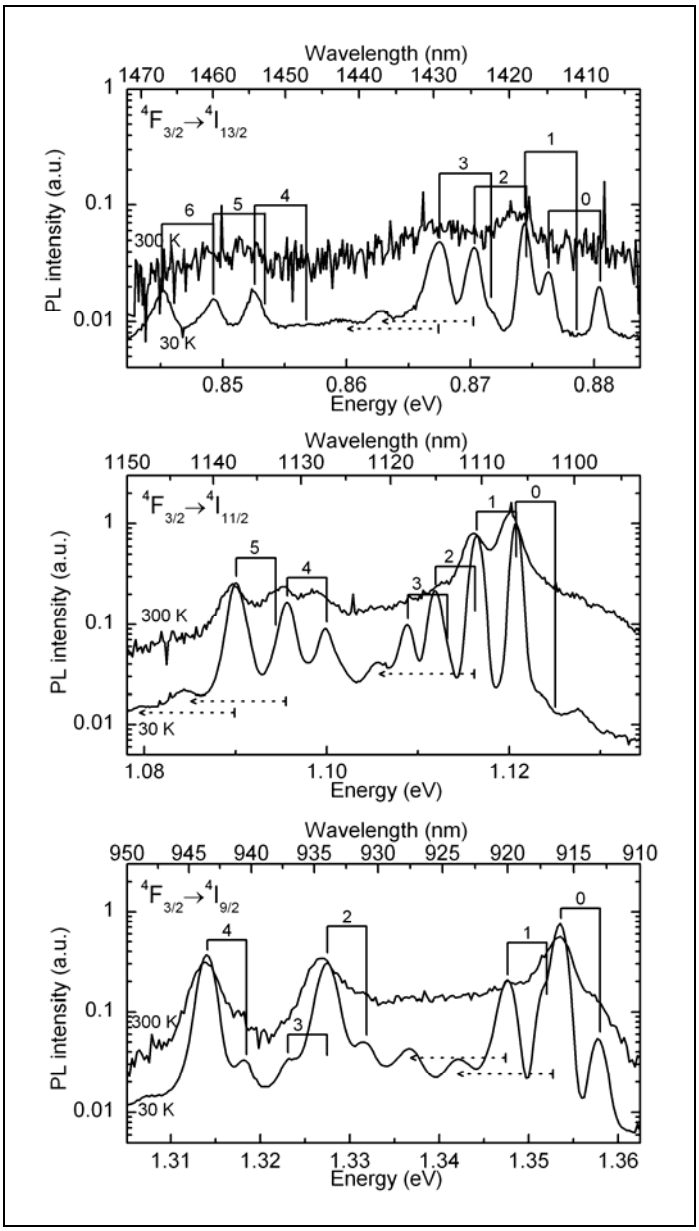

Figure 4. Room-temperature (300 K) and low-temperature (~30 K) PL spectra in logarithmic scale from GaN:Nd optically excited at 836 nm. Transitions from the lower and upper levels of the $^4F_{3/2}$ excited state to the *m*th Stark level of the $^4I_{9/2}$, $^4I_{11/2}$, and $^4I_{13/2}$ levels and RE-related (marked with an arrow) phonon sidebands are labeled.

Figure 5 shows the PL spectra in logarithmic scale from GaN:Nd optically excited below and above the bandgap at 836 and 325 nm, respectively. The above bandgap pump creates electrons in the GaN conduction band that relax primarily through non-radiative transitions, presumably through defects, to the upper Nd bands, eventually ending up in the $^4F_{3/2}$ band. In many RE-doped GaN materials, these defects aid in electron transfer to the RE atom, often leading to stronger PL emission from multiple "sites" as described by O'Donnell et al. (*15*). Moreover,

when Nd ions occupy multiple sites within the GaN matrix, the PL for above and below bandgap excitation can reveal markedly different spectra. The extra peaks marked by a downward arrow in the 325 nm spectrum in figure 5 indicate plasma lines from the 325 nm laser. Non-laser-related peaks that only appear in the above bandgap pumping PL are shaded. Disregarding the plasma lines, the PL spectra from GaN:Nd excited at 836 and 325 nm are nearly identical. These results indicate that the majority of Nd atoms sit on the same "site" within the GaN matrix, with much less influence of defect assisted transitions involving multiple "sites."

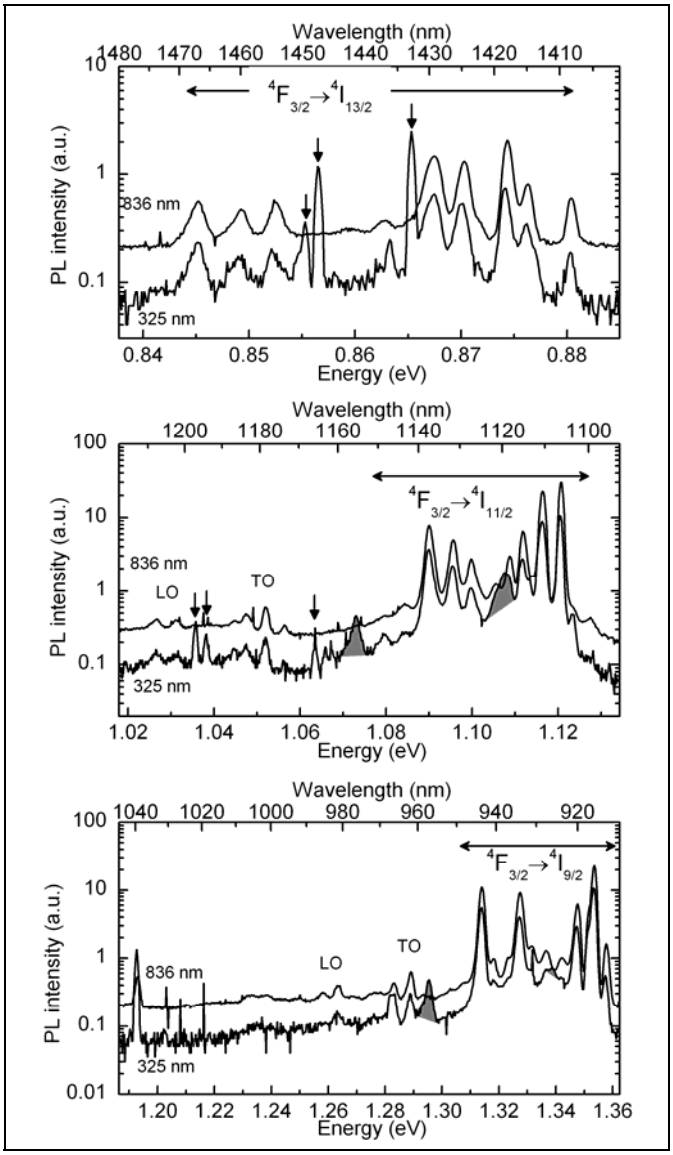

Figure 5. Low-temperature (~30 K) PL spectra in logarithmic scale from GaN:Nd optically excited below and above the bandgap at 836 and 325 nm, respectively. Longitudinal optical (LO) and transverse optical (TO) phonon sidebands are labeled. Peaks marked with a downward arrow indicate plasma lines from the 325-nm laser.

In addition to the $^4F_{3/2} \rightarrow {}^4I_{9/2}$, $^4I_{11/2}$, and $^4I_{13/2}$ transitions, weak peaks shifted lower in energy from the main peaks by 90, 64, and 11 meV are observed. The 90- and 64-meV shifts (see figure 5) agree well with the GaN LO and TO phonon energies (*16*), respectively, and are attributed to electron-phonon coupling, as observed in other RE-doped GaN materials (*17*). The 11-meV mode (see figure 4) is not observed in Raman measurements of the bulk crystal and is hence assigned to a localized mode that involves the Nd ion. A mode of similar energy (12 meV) has recently been found in the excitation-emission spectra of Eu-doped samples (*18*). From the intensity ratio of the phonon sideband peak to the relevant zero-phonon peak, we can estimate the electron-phonon coupling strength to be quite weak, having a Huang-Rhys (*19*) factor S of <0.1.

Transitions from the $^4I_{9/2}$ ground state to the upper states $^4F_{5/2}$, $^2H_{9/2}$, $^4F_{7/2}$, and $^4S_{3/2}$, between 1.46–1.54 eV (805–850 nm) and 1.58–1.62 eV (765–785 nm) are observed in PLE spectra shown in figure 6. After excitation into the upper state, the ions relax into the $^4F_{3/2}$ state, from which they can radiatively decay back into the ground state. Figure 6 displays the PLE spectra detected at the emission energy 1.12 eV (1106 nm) at ~13 and ~150 K. We compare the temperature dependent PLE spectra and assume a Boltzmann distribution of the electron population in the $^4F_{3/2}$ manifold to help identify the excitation peaks. At low temperature, we attribute the excitation peaks to transitions from the ground state and the first thermally excited state of the $^4I_{9/2}$ level to the mth Stark level of the $^4F_{5/2}$, $^2H_{9/2}$, $^4F_{7/2}$, and $^4S_{3/2}$ upper states. This assignment is consistent with the splitting found in the PL spectra between the $m = 0$ and the $m = 1$ Stark level of the $^4I_{9/2}$ manifold. PLE spectra detected at different wavelengths show the same peaks with similar intensity ratios. The strongest emission occurs at an excitation energy of 1.48 eV (836 nm). Again, phonon sidebands can be observed, which are shifted higher in energy by amounts related to the LO and TO phonons of the host material and RE-related phonons, just as observed for the PL spectra and hence confirming our assignment. Table 1 summarizes the crystal field-split level energies of Nd^{3+} ions in GaN (*20*). Additional information about transitions from the $^4I_{9/2}$ ground state to the upper states $^2G_{7/2}$ and $^4G_{5/2}$ between 1.98–2.07 eV (600–630 nm) was obtained from combined excitation-emission spectroscopy (CEES).

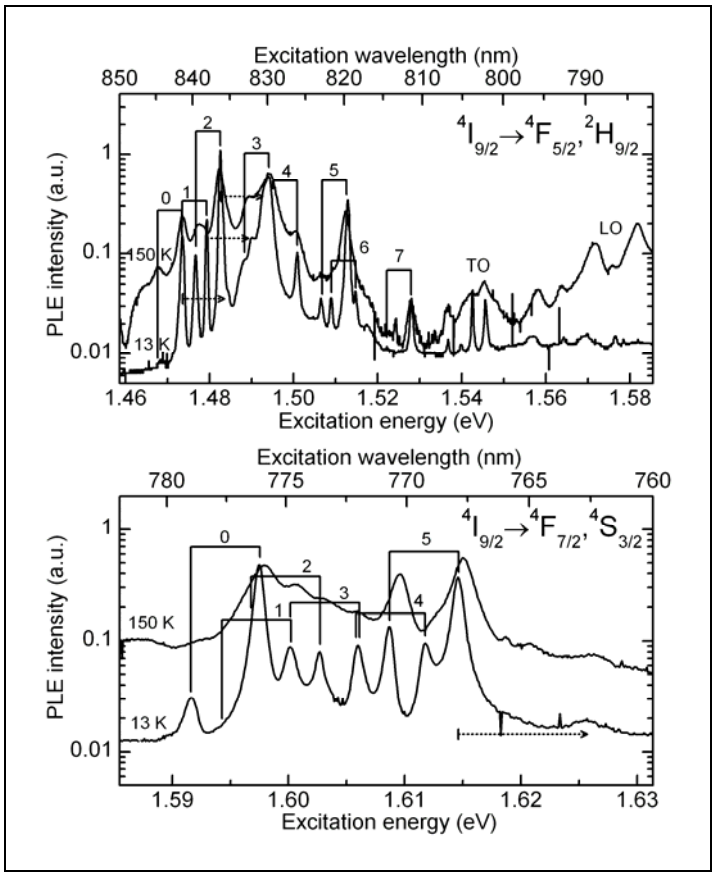

Figure 6. PL excitation spectra in logarithmic scale from GaN:Nd measured at the 1106 nm emission line at ~13 and ~150 K. Transitions from the lowest two levels of the $^4I_{9/2}$ ground state to the *m*th Stark level of the $^4F_{5/2}$, $^2H_{9/2}$, $^4F_{7/2}$, and $^4S_{3/2}$ levels, as well as LO and TO phonon replicas are labeled.

Table 1. Energy of the crystal field-split levels of Nd^{3+} ions in GaN for the main incorporation site as determined by PL, PLE, and CEES measurements.

Manifold	No. of Stark	Energy (meV)	Manifold	No. of Stark	Energy (meV)
$^4I_{9/2}$	5	0 5.9 26.1 30.4 39.5	$^4F_{5/2}$, $^2H_{9/2}$	8	1470.8 1476.6 1479.8 1491.3 1498.0 1510.0 1511.8 1525.1
$^4I_{11/2}$	6	232.8 236.8 241.6 244.7 257.9 263.5	$^4F_{7/2}$, $^4S_{3/2}$	6	1594.2 1596.9 1599.3 1602.6 1608.5 1611.2
$^4I_{13/2}$	7	477.2 479.2 483.2 486.2 501.0 504.2 508.4	$^2G_{7/2}$, $^4G_{5/2}$	7	1987.7 1998.5 2022.8 2050.4 2051.1 2056.3 2061.5
$^4F_{3/2}$	2	1353.5 1357.7			

For initial optical loss and gain measurements, a GaN:Nd sample with a Nd concentration of 0.03 at.% was etched into 750 x 460 μm structures using standard photolithography. The optical loss was measured using the shifting excitation spot (SES) technique (*21*). Optical gain was measured using the variable stripe length (VSL) method (*22*). Both loss and gain measurements were performed with above bandgap excitation at room temperature. The internal loss coefficient α was measured at the strongest emission energy 1.12 eV (1106 nm). The optical loss is related to the output intensity I by the following equation:

$$I = I_o e^{-\alpha d} \tag{1}$$

where I_o is the output intensity at the excitation spot and d is the distance between the facet and the excitation spot. A linear fit to $\ln(I/I_o)$ as a function of d gives an optical loss of $\alpha = 6.5 \pm 5$ cm^{-1} (figure 7). This loss is >3 times smaller than that reported for Eu-doped GaN (20 cm^{-1}) at an emission wavelength of 620 nm (*23*).

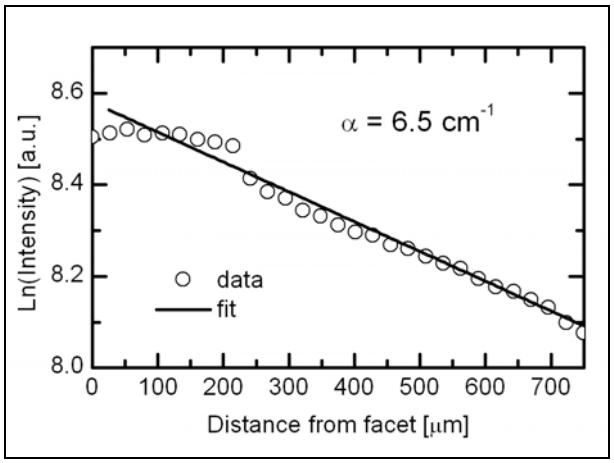

Figure 7. Optical loss at emission energy 1.12 eV (1106 nm) measured using the SES technique. The solid line is a fit of the experimental data (open circles) according to equation 1.

The relationship between output intensity I and net modal gain g_{mod} using the VSL method is given by the expression

$$I = \frac{J_o}{g_{mod}}\left(e^{g_{mod}l} - 1\right) \tag{2}$$

where J_o is the spontaneous emission intensity emitted per unit length, l is the length of the excitation beam, and g_{mod} is the net modal gain defined by $g_{mod} = \Gamma g_m - \alpha$. The variables Γ and g_m are the waveguide confinement factor and gain of the material, respectively.

Figure 8 shows the output intensity as a function of excitation length. By fitting the experimental data with equation 2, we obtain $g_{mod} = -2 \pm 5$ cm^{-1}, indicating a small gain of the material g_m. The small material gain may be due to the small Nd concentration in the waveguide structure. The discrepancy between the experimental data and the fit in figure 8 at short excitation lengths may be due to diffraction effects. More recently, 836-nm pumping experiments have been conducted on bars containing thin GaN:Nd layers of similar Nd at.%, but with aluminum gallium nitride (AlGaN) waveguide cladding layers. The same experiments have also been conducted on bars containing a SIMS stack of GaN:Nd layers with Nd at.% of 1.439, 0.057, and 0.202. The total thickness of this sample was similar to that of the sample previously investigated, and it also has no AlGaN waveguide cladding layers. No improvement in gain or loss has been achieved thus far.

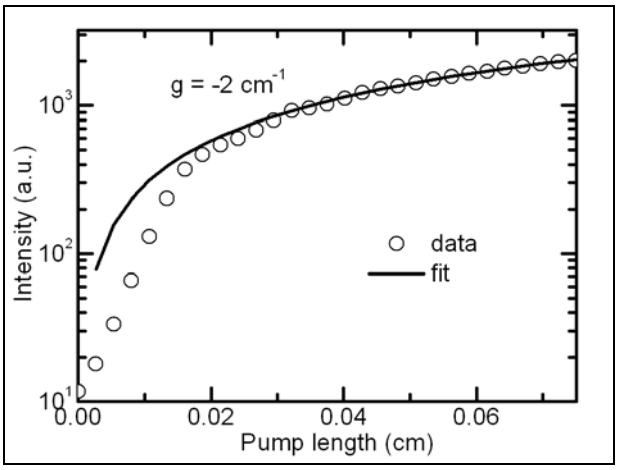

Figure 8. Output intensity versus excitation length measured at emission energy 1.12 eV (1106 nm). The solid line is a fit of the experimental data (open circles) according to equation 2.

3.3 Optical Studies of Nd Doped AlN

While GaN may be a good choice as a host for RE ion laser media because of its high thermal conductivity, wider bandgap materials such as AlN could potentially be even better RE ion laser hosts because of their higher thermal conductivity than GaN (up to 340 W/(m-K) for AlN (*24*), or 1.5 to 3 times that of GaN). To this end, Nd doping and luminescence have been investigated for AlN. Figure 9 shows the first report of characteristic luminescence spectra for in situ doping of Nd in AlN for different growth temperatures and Al fluxes, focusing on transitions from the $^4F_{3/2}$ excited state to the $^4I_{11/2}$ manifold. For a constant Nd flux, luminescence intensity increases as the growth temperature is lowered. In addition, at a given growth temperature luminescence intensity increases with decreasing Al flux and constant Nd flux. This trend is seen most clearly in the 850 °C growth data (navy and magenta lines in the plot), for which using ½ the Al flux leads to a nearly three times increase in Nd PL intensity. This trend suggests that since Al binds with N more aggressively than Ga and Nd takes the Al or Ga site, a larger Al flux suppresses Nd incorporation more so than a comparable Ga flux. In addition, the PL peak positions are shifted slightly with respect to those for Nd in GaN. For example, the dominant PL peak in AlN:Nd is red shifted by ~1 nm relative to the 1107 nm peak in GaN:Nd. However, the next largest peak (at 1111 nm in GaN:Nd) is red shifted by ~5 nm in the AlN:Nd spectra. These differences may be associated with the different crystal field experienced by the Nd in AlN, perhaps due to the larger strain associated with Nd taking the site of the smaller Al atom.

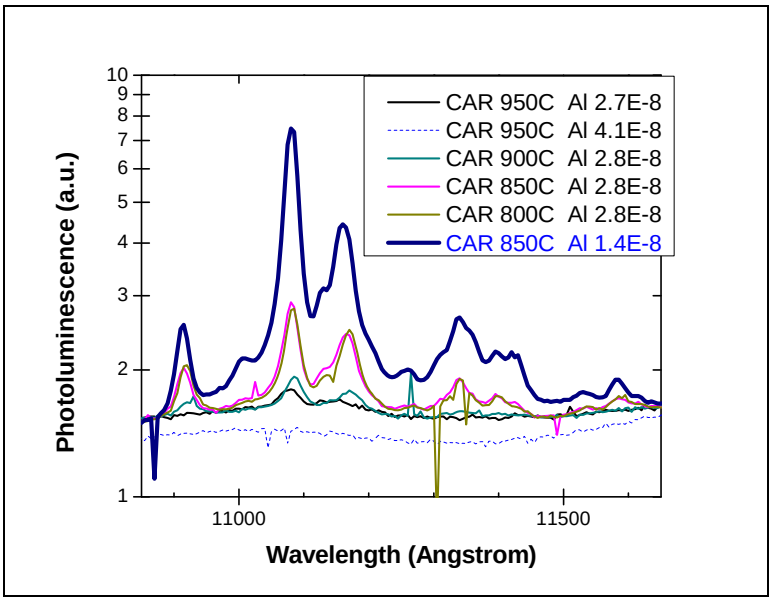

Figure 9. PL from Nd doped AlN as a function of growth temperature and Al flux for ${}^4F_{3/2}$ to ${}^4I_{11/2}$ transitions.

4. Conclusions

In conclusion, in situ Nd doping of GaN and AlN by PA-MBE has been demonstrated for the first time. For GaN, the Nd doping is controlled by the GaN growth conditions and the Nd effusion cell temperature. The Rutherford backscattering spectrometry (RBS) and SIMS data indicated Nd doping as high as ~8 at.% with no evidence of phase segregation identified by XRD for Nd up to ~1 at.%. Nd incorporation was found to reach a limit while maintaining crystal quality. Strong room-temperature luminescence corresponding to the three characteristic Nd emission multiplets was observed, with the Stark energy levels resolved by PL and PLE. Although the 4*f* electrons are well shielded from the host material, weak electron-phonon interactions are still observable. Spectral correlation of the three characteristic Nd emission multiplets for above (325 nm) and below (836 nm) GaN bandgap excitation imply enhanced substitutional doping at the Ga site. The highest room-temperature PL intensities corresponded to a doping level between 0.1–1 at.%. The enhanced substitutional doping at the Ga site and low optical loss in waveguide structures suggests that GaN:Nd with a high enough Nd concentration and number of Nd atoms, low enough structural defect density, and a high quality laser resonator with cleaved facets may have significant potential for use in simple, area-scalable, room-temperature, diode-pumped solid-state HELs. Next-generation devices may be able to take advantage of the improved thermal conductivity of an AlN host.

5. References

1. Favennec, P. N.; L'Haridon, H.; Salvi, M.; Moutonnet, D.; Leguillou, Y. *Electronic Lett.* **1989**, *25*, 718.
2. Steckl, A. J.; Zavada, J. M. *Mater. Res. Bull.* **1999**, *24*, 16.
3. Steckl, A. J.; Zavada, J. M. *Mater. Res. Bull.* **1999**, *24*, 33.
4. Koechner, W. *Solid-State Laser Engineering*; (Springer, Berlin), 5th ed., pg. 37, 1999.
5. Kim, S.; Rhee, S. J.; Li, X.; Coleman, J. J.; Bishop, S. G. *Phys. Rev.* **1998**, *B57*, 14588.
6. Kim, J. H.; Davidson, M. R.; Holloway, P. H. *Appl. Phys. Lett.* **2003**, *83*, 4746.
7. Kim, J. H.; Holloway, P. H. *Appl. Phys. Lett.* **2004**, *85*, 1689.
8. Kim, J. H.; Holloway, P. H. *J. Appl. Phys.* **2004**, *95*, 4787.
9. Kim, J. H.; Shepherd, N.; Davidson, M.; Holloway, P. H. *Appl. Phys. Lett.* **2003**, *83*, 641.
10. Readinger, E. D.; Metcalfe, G. D.; Shen, H.; Wraback, M. *Appl. Phys. Lett.* **2008**, *92*, 061108.
11. Steckl, A. J.; Heikenfeld, J. C.; Lee, D. S.; Garter, M. J.; Baker, C. C.; Wang, Y. Q.; Jones, R. *IEEE J. Sel. Top. Quantum Electron.* **2002**, *8*, 749.
12. Zou, J.; Kutchetkov, D.; Balandin, A. A.; Florescu, D. I.; Pollak, Fred H. *J. Appl. Phys.* **2002**, *92*, 2534.
13. Silkowski, E.; Yeo, Y. K.; Hengehold, R. L.; Goldenberg, B.; Pomrenke, G. S. *Rare Earth Doped Semiconductors II Symposium* **1996**, *69*.
14. Vanuiter, L. G.; Johnson, L. F. *J. Chem. Phys.* **1966**, *44*, 3514.
15. O'Donnell, K. P.; Hourahine, B. *Eur. Phys. J.-Appl. Phys.* **2006**, *36*, 91.
16. Siegle, H.; Kaczmarczyk, G.; Filippidis, L.; Litvinchuk, A. P.; Hoffmann, A.; Thomsen, C. *Phys. Rev.* **1997**, *B 55*, 7000.
17. Dierolf, V.; Sandmann, C.; Zavada, J.; Chow, P.; Hertog, B. *J. Appl. Phys.* **2004**, *95*, 5464.
18. Dierolf, V.; Fleischman, Z.; Sandmann, C.; Wakahara, A.; Fujiwara, T.; Munasinghe, C.; Steckl, A. *Mater. Res. Soc. Symp. Proc.* **2005**, *3.6.1*, 866.
19. Vanuiter, L. G.; Johnson, L. F. *J. Chem. Phys.* **1966**, *44*, 3514.

20. Metcalfe, G. D.; Readinger, E. D.; Shen, H.; Woodward, N. T.; Dierolf, V.; Wraback, M. *J. Appl. Phys.* **2009**, *105*, 053101.

21. Dal Negro, L.; Bettotti, P.; Cazzanelli, M.; Pacifici, D.; Pavesi, L. *Opts. Commun.* **2004**, *229*, 337.

22. Shaklee, K. L.; Nahory, R. E.; Leheny, R. F. *J. Lumin.* **1973**, *7*, 284.

23. Park, J. H.; Steckl, A. J. *Appl. Phys. Lett.* **2004**, *85*, 4588.

24. Perry, P. B.; Rutz, R.F. *Appl. Phys. Lett.* **1978**, *33* 319.

6. Transitions

6.1 Publications

1. Readinger, E. D.; Metcalfe, G. D.; Shen, H.; Wraback, M. GaN Doped with Neodymium by Plasma-assisted Molecular Beam Epitaxy. *Appl. Phys. Lett.* **2008**, *92*, 061108.
2. Metcalfe, Grace D.; Readinger, Eric D.; Shen, Hongen; Woodward, Nathaniel T.; Dierolf, Volkmar; Wraback, Michael. Crystal-field Split Levels of Nd^{3+} Ions in GaN Measured by Luminescence Spectroscopy. *J. of Applied Physics* **2009**, *105*, 053101.
3. Metcalfe, Grace D.; Readinger, Eric D.; Shen, Hongen; Woodward, Nathaniel T.; Dierolf, Volkmar; Wraback, Michael. Energy Levels of Nd^{3+} Ions in GaN. *Physica Status Solidi (c)* **2009**, *6*, S671.
4. Readinger, Eric; Metcalfe, Grace; Shen, Hongen; Woodward, Nate; Jha, Naveen; Dierolf, Volkmar; Wraback, Michael. GaN Doped with Neodymium by Plasma-Assisted Molecular Beam Epitaxy for Potential Lasing Applications. In *Rare-Earth Doping of Advanced Materials for Photonic Applications*, Dierolf, V.; Fujiwara, Y.; Hommerich, U.; Ruterana, P.; Zavada, J., eds., *Mater. Res. Soc. Symp. Proc.* Vol. 1111**,** Warrendale, PA, 2009, 1111-D-02-04 (invited paper).
5. Dierolf, Volkmar; Woodward, Nate; Jha, Naveen; Metcalfe, Grace; Readinger, Eric; Wraback, Michael. Spatially Resolved Site Selective Optical Spectroscopy on Nd Doped GaN Epitaxial Layers. In *Rare-Earth Doping of Advanced Materials for Photonic Applications*, edited by Dierolf, V.; Fujiwara, Y.; Hommerich, U.; Ruterana, P.; Zavada, J., eds., *Mater. Res. Soc. Symp. Proc*, Vol. 1111, Warrendale, PA, 2009, 1111-D-02-06.

6.2 Presentations

1. Readinger, Eric D.; Metcalfe, Grace D.; Shen, Paul; Wraback, Michael; Jha, Naveen; Woodward, Nathaniel; Dierolf, Volkmar. Plasma-assisted Molecular Beam Epitaxial Growth of (Al)GaN Doped with Neodymium for Potential Lasing Applications. *Impurity Based Electroluminescent Devices and Materials*, Tossa De Mar, Spain, October 2009.
2. Metcalfe, G. D.; Readinger, E. D.; Shen, H.; Woodward, N. T.; Dierolf, V.; Wraback, M. Energy levels of Nd^{3+} ions in GaN. *International Workshop on Nitride Semiconductors*, Montreaux, Switzerland, October 2008.

3. Readinger, Eric; Metcalfe, Grace; Shen, Hongen; Woodward, Nate; Jha, Naveen; Dierolf, Volkmar; Wraback, Michael. GaN Doped with Neodymium by Plasma-Assisted Molecular Beam Epitaxy for Potential Lasing Applications. *MRS Fall Meeting*, Boston, MA, December 2008 (invited).
4. Dierolf, Volkmar; Woodward, Nate; Jha, Naveen; Metcalfe, Grace; Readinger, Eric; Wraback, Michael. Spatially Resolved Site Selective Optical Spectroscopy on Nd Doped GaN Epitaxial Layers. *MRS Fall Meeting*, Boston, MA, December 2008.

List of Symbols, Abbreviations, and Acronyms

AlGaN	aluminum gallium nitride
AlN	aluminum nitride
BEP	beam equivalent pressure
CEES	combined excitation-emission spectroscopy
CL	cathodoluminescence
CW	continuous wave
DEW	directed energy weapon
Dy	dysprosium
EL	electroluminescence
Er	erbium
Eu	europium
FWHM	full width at half maximum
GaN	gallium nitride
Ge	germanium
HeCd	helium-cadmium
HEL	high-energy laser
LO	longitudinal optical
Nd	neodymium
PA-MBE	plasma-assisted molecular beam epitaxy
PL	photoluminescence
PLE	photoluminescence excitation
Pr	praseodymium
RBS	Rutherford backscattering spectrometry
RE	rare earth

RT	room temperature
SES	shifting excitation spot
SIMS	secondary ion mass spectrometry
Tm	thulium
TO	transverse optical
VSL	variable stripe length
XRC	x-ray rocking curve
XRD	x-ray diffraction
YAG	yttrium aluminum garnet
Yb	ytterbium
YLF	yttrium lithium fluoride
YVO_4	yttrium orthovanadate

COPIES ORGANIZATION

1 (PDF only) DEFENSE TECHNICAL INFORMATION CTR
DTIC OCA
8725 JOHN J KINGMAN RD
STE 0944
FORT BELVOIR VA 22060-6218

1 CD DIRECTOR
US ARMY RESEARCH LAB
IMNE ALC HRR
2800 POWDER MILL RD
ADELPHI MD 20783-1197

1 CD DIRECTOR
US ARMY RESEARCH LAB
RDRL CIM L
2800 POWDER MILL RD
ADELPHI MD 20783-1197

1 CD DIRECTOR
US ARMY RESEARCH LAB
RDRL CIM P
2800 POWDER MILL RD
ADELPHI MD 20783-1197

3 CDS DIRECTOR
US ARMY RESEARCH LAB
RDRL SEE
L BLISS
RDRL SEE M
M WRABACK
RDRL SEE O
M DUBINSKY
2800 POWDER MILL RD
ADELPHI MD 20783-1197

ABERDEEN PROVING GROUND

1 CD DIR USARL
RDRL CIM G (BLDG 4600)

TOTAL: 8 (1 ELEC, 7 CDs)